DOI 10.1515/aot-2012-0081 — Adv. Opt. Techn. 2013; 2(2): 147–157

Review Article

Markus Strobel[a,*] and Dietmar Döttling[b]

High dynamic range CMOS (HDRC) imagers for safety systems

Abstract: The first part of this paper describes the high dynamic range CMOS (HDRC®) imager – a special type of CMOS image sensor with logarithmic response. The powerful property of a high dynamic range (HDR) image acquisition is detailed by mathematical definition and measurement of the optoelectronic conversion function (OECF) of two different HDRC imagers. Specific sensor parameters will be discussed including the pixel design for the global shutter readout. The second part will give an outline on the applications and requirements of cameras for industrial safety. Equipped with HDRC global shutter sensors SafetyEYE® is a high-performance stereo camera system for safe three-dimensional zone monitoring enabling new and more flexible solutions compared to existing safety guards.

Keywords: CMOS image sensor; global shutter; high dynamic range CMOS (HDRC); safe camera system; SafetyEYE.

OCIS codes: 110.4850; 150.6910; 150.5495; 150.5758; 100.6890.

[a]Markus Strobel is the author of section 2 and the associated topics on CMOS image sensors in this paper.
[b]Dietmar Döttling is the author of section 3 and the associated topics on safety systems in this paper.
***Corresponding author: Markus Strobel**, Institut für Mikroelektronik Stuttgart (IMS CHIPS), Allmandring 30a, 70569 Stuttgart, Germany, e-mail: strobel@ims-chips.de
Dietmar Döttling: Pilz GmbH & Co. KG, Felix-Wankel-Straße 2, 73760 Ostfildern, Germany

1 Introduction

With advances in the field of digital image acquisition and processing, previously impossible or difficult to dissolve applications have been enabled especially through the progress in today's CMOS imager technology. Camera based safety systems and related applications such as automotive driver assistance systems largely rely on valid image data independent of environmental illumination conditions. Therefore, the image sensor is a key element to ensure reliable system performance and operational availability. Figure 1, captured by a high dynamic range CMOS (HDRC®) imager, gives a glimpse of the very high brightness range of a scene the imager is facing. In industrial environments, similar challenges arise. Section 2 introduces shutter type and optoelectronic properties of these CMOS sensors.

Being a high performance stereo camera system for safe three-dimensional (3D) zone monitoring, SafetyEYE® is equipped with HDRC global shutter sensors for high dynamic range (HDR) image acquisition. Work practices will become more efficient the closer man and machine work together. Static or 1D protective devices, such as guards, frequently reach their limits. Safe camera systems overcome these limits opening up new possibilities. However, the specifications relating to safety must be met. This will be addressed in Section 3.

2 Logarithmic high dynamic range CMOS (HDRC) imagers

HDRC imagers, their properties, technology and applications have been intensively discussed in previous articles and publications [1–5]. The following part of this paper focuses on the shutter types: rolling shutter (RS) versus global shutter (GS). The next paragraph will introduce the two HDRC imagers. Both chips are available in a 48-pin ceramic package shown in Figure 2. The GS function is an important feature for the camera system for safe 3D applications, described in Section 3.2 which requires the simultaneous sampling of the image information of three synchronized image sensors at the same time.

As the two imagers are built using similar functional blocks some of the main specifications listed in Table 1 are

Figure 1 High dynamic range scene captured with a HDRC® image sensor in an automotive application with extreme brightness conditions.

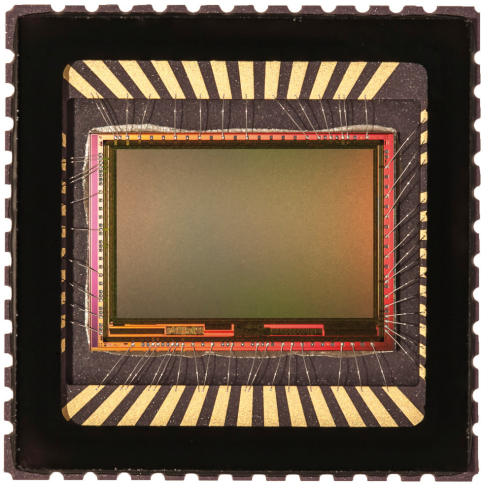

Figure 2 Logarithmic HDRC image sensor assembled in a LCC48 ceramic package with lid glass.

Table 1 Main specification of the logarithmic HDRC-VGAy and HDRC-G2 image sensors with rolling and global shutters, respectively.

Parameter	Unit	HDRC-VGAy	HDRC-G2
Shutter type	–	Rolling shutter	Global shutter
Sensor format	inch	2/3	2/3
Diagonal	mm	9.14	9.24
Dynamic range (DR)	dB	>170	>130
Resolution	Pixel	768×496	772×507
Region of interest (ROI)	Pixel	Down to 2×2	Down to 2×2
Pixel size	μm^2	10×10	10×10
Fill factor	%	>40	>25
Pixel clock	MHz	12	12
Frame rate full frame	Hz	30	30
ROI 100×100 pixel	Hz	1000	1000
On-chip ADC	Bit	10	10
Power supplies	V	2.5/3.3	2.5/3.3

nearly identical, such as sensor format and resolution, pixel size and readout clock, frame rate and bit depth of the on-chip analog-to-digital converter (ADC). Both have a logarithmic optoelectronic conversion function (log OECF) for HDR image acquisition. Region-of-interest (ROI) readout is supported by user-defined register settings via a serial digital control interface of the sensors.

2.1 Global shutter versus rolling shutter

The main difference between the imagers in Table 1 is the type of pixel cell which determines the shutter functionality: RS or GS. Figure 3 schematically shows the extension of a RS to a GS pixel cell with the sample and hold (S&H) circuit consisting of a switch transistor $M_{shutter}$, a hold capacitance C_{hold} and a second buffer. For the GS pixel cell, the fill factor is decreased due to a S&H circuitry added inside the pixel, thus lowering the available area for the photodiode. The logarithmic compression to handle the high dynamic range of photocurrents is already achieved at the beginning of the signal chain. Transistor M_{log}

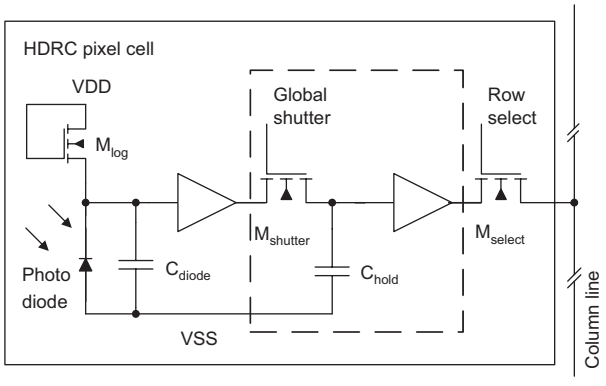

Figure 3 Logarithmic HDRC pixel cell (schematic). With the additional S&H circuitry (dashed box), the standard RS pixel is extended with GS functionality.

operating in the subthreshold region continuously converts the photocurrent into its drain-source voltage proportional to the logarithm of the illuminance – without the need to set an integration time in contrast to linear active pixel sensors.

For CMOS image sensors, RS is the standard method to read out image information of the pixel array [6]. Each pixel row is addressed sequentially by asserting the row select signal (transistor M_{select}) and then multiplexing the column lines to an on-chip (or external) ADC before the next row is addressed. In doing so, a certain time is required between the first and the last row of the pixel array being read out. This also determines the maximum frame rate of the sensor as the reciprocal of the readout time (including line and frame synchronization pauses). At 30 frames/s, the delay time between the first and the last row is approximately 33 ms. For scenes with a moving object, this delay time results in a geometrically distorted image when captured with an RS sensor. To omit this effect, the additional S&H circuitry of the GS sensors samples the scene information simultaneously for all pixels in the array by asserting the GS signal for a very short time (microseconds) before the row-by-row readout starts [7]. Independent of scene movements, the delay time now only affects the hold capability of the S&H circuitry. This will be discussed in the following paragraphs by means of the OECF.

Captured images in Figure 4 clearly depict the advantage of the GS over the RS imager with objects moving at high speed. The fact that for a stereo camera system only small geometric distortions will affect the determined displacement of objects in stereo images and lower the accuracy in the calculated depth map is not so obvious, but equally important.

2.2 Optoelectronic conversion function (OECF)

The digital output of the sensor or gray value y in digital numbers (DNs) in relation to illuminance E (or irradiance) at the sensor plane is described and measured by the OECF formula $y=f(E)$. A general overview of measurement setup and methods is given by the EMVA1288 standard [8]. The illumination source used here for the OECF measurements has a color temperature of 5650 K in contrast to the narrowly monochromatic irradiance defined in the standard. Therefore, photometric units (lx) instead of radiometric units (W/m^2) are measured here for illuminance E.

Figure 5 shows the block diagram of the logarithmic OECF from the irradiated photodiode with illuminance E followed by logarithmic compression, buffers and amplifiers subsumed by amplification G and finally ADC with digital output $y(E)$. An optional S&H circuit in the case of GS would be inserted just after logarithmic compression.

With the evaluation camera systems [9, 10] for grabbing digital images and a homogeneous illumination equipment, the OECFs of the RS and GS sensors have been measured with a frame size of 480 rows and 280 columns at rate of 50 frames/s. The plotted digital gray value in Figure 6 is the arithmetic mean value of all pixels $\mu_y=\bar{y}(E)$ as defined by EMVA1288 [8].

The OECF of the RS sensor can be mathematically modeled by Eq. (1) associated with the notation introduced in [11] which is related to EMVA1288 [8].

The three sensor parameters are dark level y_{dark} in DN, logarithmic overall system gain K in DN/decade, and photodiode dark current equivalent illuminance E_d in lx (or W/m^2). Note: in the literature sometimes the natural

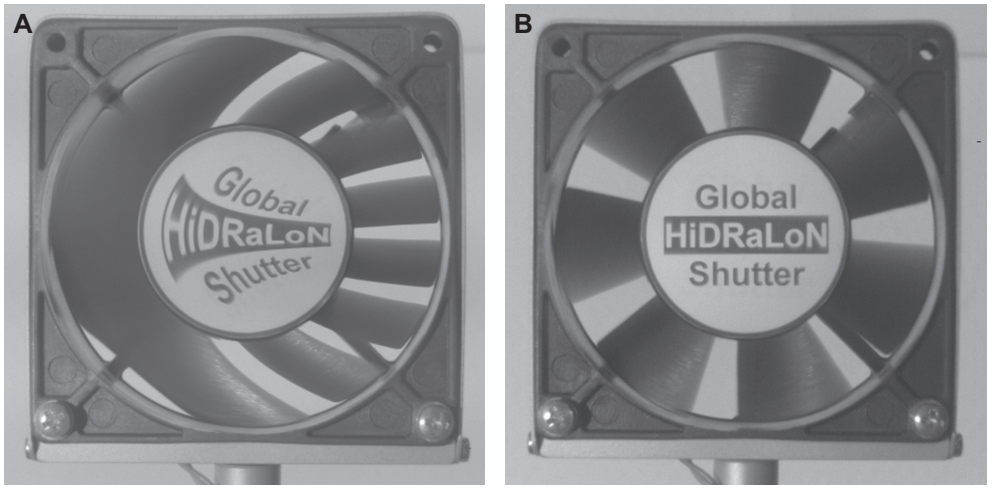

Figure 4 Rotating fan at high speed: (A) geometric distortion due to the RS readout, (B) distortion free image acquisition with the GS sensor.

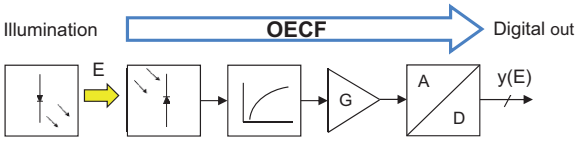

Figure 5 Measured OECF gives digital output of a sensor as a function of illuminance *E*.

logarithm (ln) is used for the OECF instead of the logarithm to the base 10. In that case, parameter *K* has to be multiplied by factor 1/ln (10)≈0.434.

$$y_{RS}(E)=y_{dark}+K\cdot\log\left(\frac{E+E_d}{E_d}\right) \quad (1)$$

For the OECF of the GS sensor given in Eq. (2) an additional linear term E/E_b had to be added to Eq. (1) which represents the effect of a parasitic photodiode of the S&H circuit at high illuminance levels. The definition of the fourth sensor parameter, bright illuminance E_b in lx (or W/m²), and the pre-factor K/ln (10) will be argued by the logarithmic derivative $dy/d\lg E$ of the OECF (log slope). E_b defines a non-strict limit for the maximum illuminance of a GS sensor.

$$y_{GS}(E)=y_{dark}+K\cdot\log\left(\frac{E+E_d}{E_d}\right)+\frac{K}{\ln(10)}\cdot\frac{E}{E_b} \quad (2)$$

The logarithmic derivative of the OECF $dy/d\lg E=\ln(10)\cdot E\cdot dy/dE$ is calculated from Eq. (1) for the RS sensor, see Eq. (3), and from Eq. (2) for the GS sensor, see Eq. (4).

$$\frac{d}{d\lg E}y_{RS}(E)=K\cdot\frac{E}{E+E_d} \quad (3)$$

$$\frac{d}{d\lg E}y_{GS}(E)=K\cdot\frac{E}{E+E_d}+K\cdot\frac{E}{E_b} \quad (4)$$

Form Eq. (3) one can find that if $E=E_d$ the log slope equals $K/2$ and from Eq. (4) if $E=E_b$ the log slope equals $2\cdot K$ under the premise that $E_d \ll E_b$. In between these two characteristic illuminance levels $E_d \ll E \ll E_b$ the log slope reaches the constant plateau value K.

For both sensors the dark random noise of the pixel (given as standard deviation σ_y according to EMVA1288 [8]) related to a full decade swing equals to $RN_{dark}/K\approx 1.1\%$. The minimum illuminance E_{min} at SNR=1 where $y(E_{min})=y_{dark}+RN_{dark}$ can be calculated with the inverse OECF function $E=f^{-1}(y)$ using Eq. (1) or Eq. (2). The low light sensitivity corresponds to a minimum illuminance $E_{min}=E_d\cdot(10^{0.011}-1)\approx E_d/39$ and a log slope at E_{min} of $(dy/d\lg E)_{min}=K(1+E_d/E_{min})^{-1}\approx K/40$ with Eq. (3) or Eq. (4). With this the dynamic range (DR)=20 log (E_{max}/E_{min}) can be calculated.

To confirm these conclusions and to determine the OECF parameters K and E_d for the RS sensor and K, E_d, E_b for the GS sensor the numerical calculated log derivative of the measured OECF data is plotted in Figure 7.

The graphically extracted parameters from Figure 6 (y_{dark} at E=1mlx$\ll E_d$) and Figure 7 (K at the plateau of the slope, E_d at $K/2$ and E_b at $2\cdot K$) are listed in Table 2 together with the deduced low light sensitivity $E_{min}=E_d/39$, the

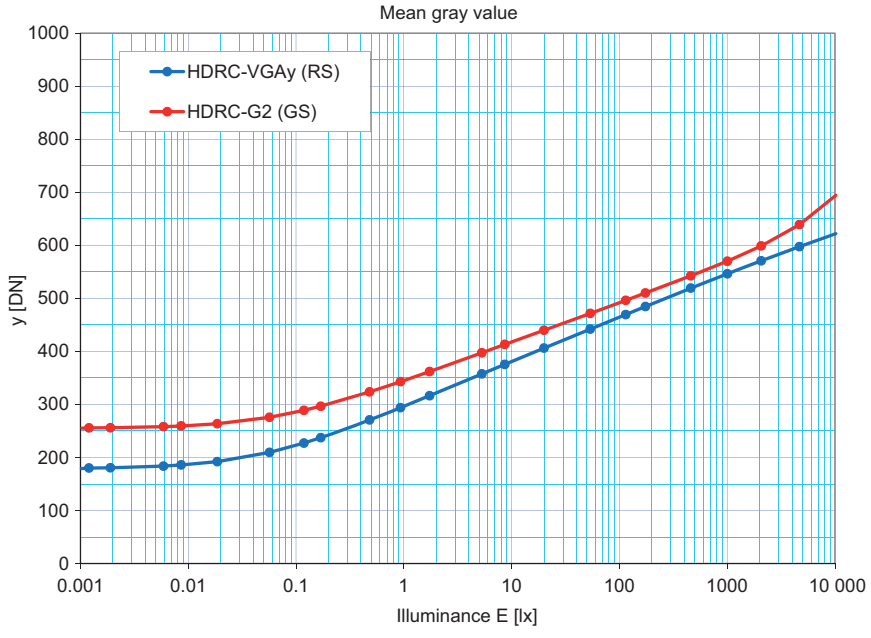

Figure 6 Measured sensor characteristics (OECF) of RS and GS sensors at 50 frames/s (10 bit digital output).

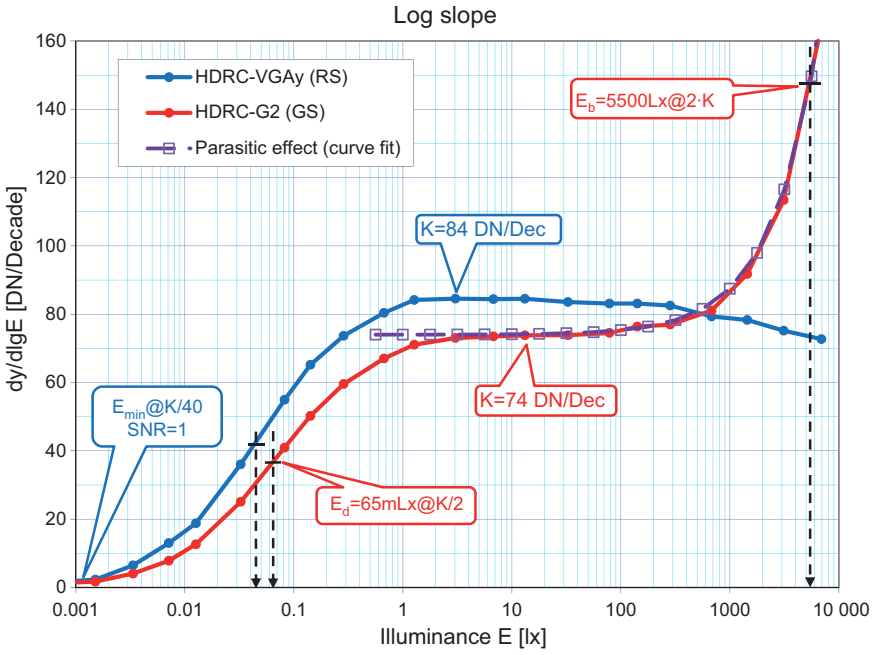

Figure 7 Calculated derivative $dy/d\lg E$ of OECF (log slope) of RS and GS sensors at 50 frames/s. Fitted curve approximates the effect of the parasitic photodiode of the S&H circuitry in the case of the GS sensor.

maximum illuminance E_{max} and the calculated DR for both sensors.

2.3 Discussion of the integrated S&H circuitry of the GS pixel

As expected, the sensor with the RS pixel has a better low light sensitivity E_{min} compared to the GS pixel due to the higher photodiode fill factor (Table 2). The logarithmic system gain K depends on the total gain G of the analog signal chain and can be adjusted in the GS sensor by a programmable gain amplifier to adapt to different DR requirements. But parameters E_{min}, E_d, E_b are gain-invariant. The validation of the additional linear term in Eq. (2) for the parasitic effect in the case of the GS sensor can be seen in Figure 7 by the well-fitted curve $K(1+E/E_b)$ representing Eq. (4) for $E \gg E_d$. With the fit parameters K=74 DN/Dec and E_b=5500 lx it has a close congruency to the numerical calculated log slope of the measured OECF.

Figure 8 depicts the integrated S&H circuitry (dashed box) inside the GS pixel cell. The small parasitic photodiode is formed by the pn junction of the source diffusion of the $M_{shutter}$ transistor. The parasitic photo current $i_{ph,parasitic}$ discharges the hold capacitor C_{hold} in hold operation during the row-by-row readout of the pixel array. The discharge current linearly depends on the parasitic photodiode sensitivity and the irradiance itself as it is generated by penetrated and stray light and diffusing electrons generated in the bulk silicon. In general, for GS sensors

Table 2 Extracted parameters for the HDRC-VGAy (RS) and HDRC-G2 (GS) sensors from OECF measurements at 50 frames/s.

Parameter	Unit	HDRC-VGAy	HDRC-G2
Shutter type	–	Rolling shutter	Global shutter
Dark level y_{dark}	DN	180	256
Logarithmic system gain K	DN/Decade	84	74
Dark illuminance E_d (log slope=K/2 due to photodiode dark current)	lx	0.045	0.065
Bright illuminance E_b (log slope=2·K due to parasitic photodiode)	lx	–	5500[b]
Low light sensitivity E_{min} (log slope=K/40, SNR=1)	lx	0.0012	0.0017
Max. illuminance E_{max}	lx	>370 000[a]	5500[b]
Dynamic range, DR (log ration of E_{max}/E_{min})	dB	>170[a]	130

[a]Illuminance>10 000 lx by directly illuminating the sensor from the fiber tail of the light source.
[b]Limited by E_b of the parasitic photodiode of the S&H circuitry, E_b depends on readout time.

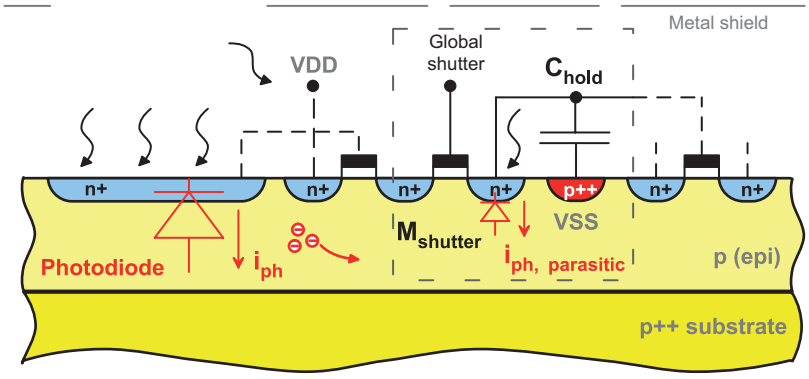

Figure 8 Detail of a GS pixel cell showing the S&H circuitry (dashed box) with the small parasitic photodiode discharging the hold capacitor C_{hold}.

the ratio $i_{ph}/i_{ph,parasitic}$ is called shutter efficiency limiting the GS function at high illuminance levels.

The voltage drop at the capacitor Δv_{drop} is therefore proportional to stray sensitivity $s_{parasitic}$ in A/lx (or $AW^{-1}m^2$), irradiance E in lx (or W/m^2), and hold time t_{hold} in s and inverse to the hold capacitor C_{hold} in F, see Eq. (5). Spectral dependencies are omitted here for simplicity.

$$\Delta v_{drop} = s_{parasitic} \cdot E \cdot t_{hold} \cdot C_{hold}^{-1} \tag{5}$$

As E_b is extracted from measurements of the mean gray value $\bar{y}(E)$, the average delay time $\bar{t}_{hold}$ between the GS pulse to the readout of the pixel rows (from first to last row) has to be considered. It is roughly half of the readout time $\bar{t}_{hold} \approx \frac{1}{2} T_{readout} \approx 1/(2 \cdot f_{frame\ rate})$ and normally shorter than the reciprocal of the frame rate. With this and the dependency, Eq. (5), in comparison to the linear term in Eq. (2) the quantity Eq. (6) for the bright irradiance E_b can be given. With a frame rate of 30 and 50 frames/s the change of E_b has been confirmed to follow this behavior.

$$E_b \sim C_{hold} \cdot f_{frame\ rate} \cdot s_{parasitic}^{-1} \tag{6}$$

Countermeasures in the pixel design to increase E_b can be addressed from Eq. (6) as increasing hold capacitor, decreasing readout time and lowering the stray sensitivity by reducing stray light and penetrating light through appropriate shielding and omitting the absorption of diffusing electrons in the pn junction of the parasitic photodiode.

2.4 Current sensor developments

Within the HiDRaLoN project [12], High Dynamic Range and Low Noise CMOS-Image-Sensors, a 3-year European project under the CATRENE research frame program, IMS CHIPS and Pilz developed and evaluated the next generation of HDR CMOS (HDRC®) imagers for camera-based safety systems, respectively.

Based on the results of a test chip with 5 µm and 7 µm pixel cells, IMS CHIPS designed a final full resolution HDRC® image sensor (currently being fabricated) with 1296×1092 pixels (1.4 mega pixels) with an optimized 6.7 µm pixel cell. This corresponds to an optical format of 2/3″ or an image diameter of 11 mm at a SXGA resolution of 1280×1024 pixels. The imager supports both RS and GS readout modes at frame rates of up to 60 frames/s. The user can select by register either the GS readout with a dynamic range >110 dB (expected) for high-speed applications or the RS mode for highest brightness dynamics of >140 dB (expected). Target applications for the new imager in addition to the camera-based safety system are automotive technologies, medical, automation and industrial applications, for example, welding process monitoring and control.

3 Applications in safety systems

3.1 Safety in industrial environment

The classic way to achieve safety in industry is to surround plant and machinery with various safeguards. Conventional safety solutions are comparably 1D in their reaction behavior: if a safety gate is opened without authorization or an operator approaches a hazardous movement, an immediate emergency stop will always result. A differentiated evaluation of the actual risk potential is impossible with such systems. When optoelectronic media are used for safety gate systems, a wide range of different sensors must also be installed, wired and aligned. This is where the wiring and installation work, plus the costs, soon add up.

For dynamic safety concepts, sensors must be able to assess events in a clearly graduated manner. With

productivity continually increasing, it must be possible to work within defined detection zones in a plant, without disrupting the whole production process (Figure 9).

Such applications require complex sensors, which can supply and also process as full information as possible from the environment. These include camera systems, for example. Camera systems have long been used in various industrial sectors for monitoring tasks as well as quality control measurements. However, for camera systems to be used in the field of safe automation, they must satisfy normative specifications.

The Machinery Directive 2006/42/EC [13] is the central specification for the design of safety-related control systems in the field of machinery safety. Put simply, the Machinery Directive governs the obligation of safety objectives to operate a safe machine.

IEC 61496 [14] with its various parts applies specifically for protective devices such as safety light curtains or camera systems, for example. It describes relevant requirements specific to optical sensors, so that the sensor itself is safe under the terms of the Machinery Directive. However, the more complex the sensor, the more costly and difficult it is to comply with the safety-relevant specifications.

3.2 Safety requirements for camera systems

SafetyEYE from Pilz is a safe, camera-based 3D protection system for zone monitoring and essentially consists of a sensing device and an analysis unit. The sensing device is installed at a height of some meters above the process. Uninterrupted monitoring from above renders all the previous, conventional floor-based mechanical safeguards superfluous (Figure 10).

The SafetyEYE operating principle can be described as follows: three camera modules equipped with a HDRC GS sensor, similar to the HDRC-G2 in Table 1 but with additional on-chip test structures, are arranged on a metal base plate to form two orthogonal stereo bases. The so-called sensor unit provides simultaneous sampled image data from the monitored zone. The analysis unit receives the data via fiber optic cable and uses it to calculate a 3D image. The images taken from three different perspectives are superimposed, enabling all objects within the field of vision to be physically perceived and precisely located. The monitoring system compares this information with predefined virtual warning and detection zones as part of each cycle (at least every 50 ms). The total system reaction time is at minimum 165 ms and the system is designed to detect human bodies up to 7.5 m.

Figure 9 Operator safety must still be guaranteed in a working environment in which the work areas of man and machine increasingly overlap. Static or 1D protective devices reach their limits in such scenarios.

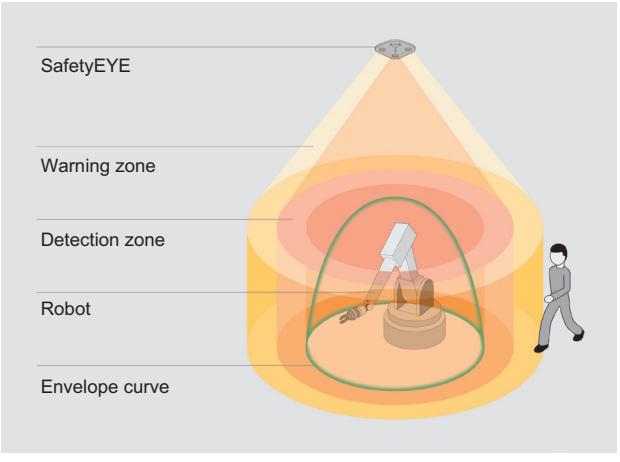

Figure 10 The safe camera system detects and reports objects that encroach into warning and detection zones. The application options for such solutions are many and varied, far exceeding the options available on previous systems.

The illumination level defined in standards and regulations for human work places (approximately 300 lux) is sufficient to allow a stable operation of the system without additional illumination.

Zone definition is software-based, using a configurator. Several virtual warning or detection zones can be arranged around the object to be monitored (Figure 11). Each one of these zones is linked to an action in the case of encroachment. If the camera system identifies that the detection zone has been encroached, the predetermined action is carried out immediately: for example, should anyone enter an area defined as a warning zone, SafetyEYE issues a visual and/or acoustic warning or slows down the movements of the machine or robot. The safety system will not initiate an immediate emergency stop until an operator enters a robot's operational range, which is defined as a detection zone.

As a camera system, SafetyEYE must meet fault detection requirements in accordance with the standard IEC 61496 [14]. With an electro-sensitive protective device in accordance with type 3 of this standard, a single fault shall not lead to the loss of the safety function. Consequently, any faults must not only be detected but also managed by the system.

The sensor uses patented test structures developed by Pilz to actively test the function of the sensor. Data are transferred from the sensing device to the analysis unit via fiber optics, so that interference from electromagnetic irradiation is excluded. Special mechanisms are applied as the data are transferred, reducing the possibility of common cause failures. Internal system tests check the function of all key software and hardware components as part of each cycle (every 50 ms). The 3D data calculation is performed safely through two diverse stereo algorithms. The whole analysis unit also has a dual-channel design.

SafetyEYE also checks the environmental conditions: bad or unfavorable light conditions such as glare from spotlights, darkness, steam and smoke must not be allowed to compromise safety. The system actively checks and detects any interference affecting the sensor head using reference markers, which are distributed within the visible range. Patented tests check whether any part of the monitored scene is concealed by objects close to the sensing device, such as hanging cables, for example.

It is also important to ensure that the angle of vision of the sensing device does not change, and thereby the set detection zones. The system also checks this with the reference markers.

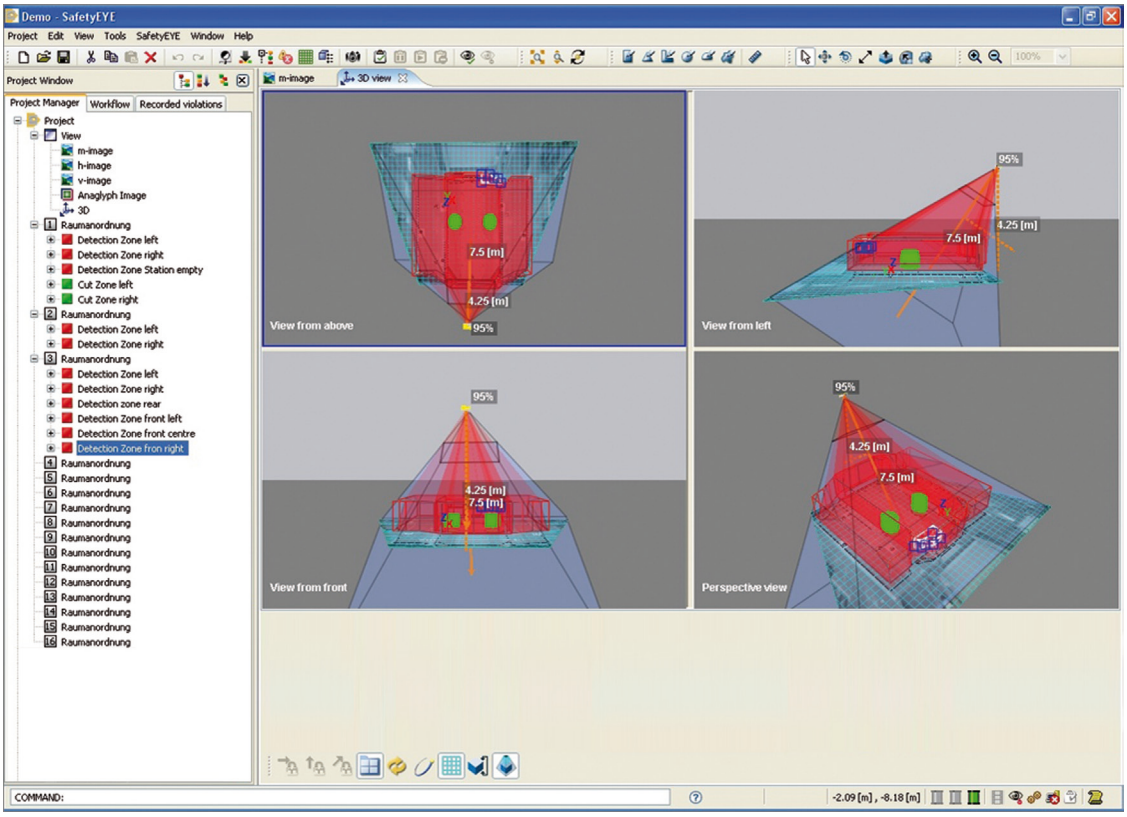

Figure 11 Warning and detection zones can be configured via software on the PC. Both the analysis unit and the programmable safety system can be programmed via Ethernet, which serves as the interface to the machine control system.

Owing to this guarantee, plus some additional safety measures, SafetyEYE is the first certified, BG-approved [15], stereoscopic camera system for series use.

3.3 3D technology creates new opportunities

As all previous, conventional floor-based safeguards are removed, innovative workplace concepts are needed, particularly in those areas where man and machine have to cooperate closely [16]. A new feature on 3D cameras is the definition of detection and warning zones of any form, in any position within the monitorable zone of the camera. Beyond the pure safety function, they also enable process conditions to be recorded and monitored. In car production, for example, a gate might be detected that is open when it actually should be closed.

It is also possible to use warning zones as 'virtual switches', for control functions, for example. With a sophisticated arrangement of warning and detection zones and, if necessary, chronological evaluation of this arrangement, it is possible to distinguish between man and machine, based on the application (Figures 12 and 13).

This enables new types of robot applications: by combining a safe robot with a safe 3D camera system, it is possible to merge a variety of strictly separate process steps. The safe robot is safely aware of its position, speed and direction of movement; the safe camera system knows the position of objects (people) around the operating range of the robot. Instead of a rigid shutdown, in future the whole system can react much more flexibly, avoid unnecessary downtimes and thus increase plant productivity.

Figure 12 With a sophisticated arrangement of warning and detection zones and, if necessary, chronological evaluation of this arrangement, it is possible to distinguish between man and machine, based on the application.

Platen presses and punching machines are another important application area. When the press is opened, all detection zones above the platen are deactivated, so a detection zone violation would not cause the opening movement to stop. An additional detection zone above the platen press housing is intended to react to anyone approaching the machine from the rear. This detection zone is active both on opening and closing. The areas to the right and left of the platen press are also safeguarded through defined detection zones. These prevent anyone from approaching or leaning into the closing platen from the side, beyond a tolerable limit. Removing the need for mechanical safeguards or fixed enclosures offers greater flexibility and increases productivity.

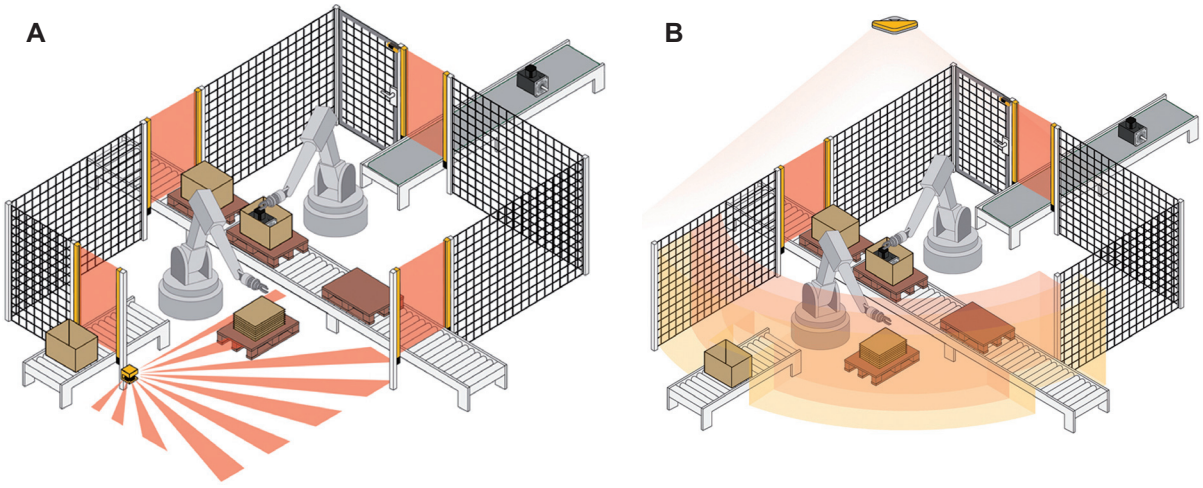

Figure 13 By combining a safe robot with a safe 3D camera system, a variety of strictly separate process steps can be merged (B) compared to mechanical safeguards or fixed enclosures (A).

Further SafetyEYE application examples are the flexible manufacturing of fuel cells [17] and a robot welding station in the automotive industry [18].

4 Conclusion

The measurements of the OECF of the two different HDRC imagers confirmed the validity of the mathematical models introduced in Section 2. It also showed a powerful DR of 170 dB and 130 dB DR for RS and GS, respectively. The given definition of bright illuminance E_b in the case of a GS sensor turned out to be a practical figure of merit for maximum illuminance which can be easily extracted from measurement data.

SafetyEYE exploiting HDR image acquisition capability of the HDRC sensors with GS for stereo vision enables new solutions for safe 3D zone monitoring. On more complex production processes, particularly in places where man and machine have to interact closely, fixed enclosures or other inflexible mechanical equipment are increasingly outdated. They disrupt the production process many times over, inciting operators to defeat what in principle are sensible safeguards.

The applicable standards must still be considered when using camera systems for safety tasks. The more complex the sensor, the more costly and difficult it is to comply with the safety-relevant specifications. This is a particular reason why safe camera technology is still in its infancy. SafetyEYE is the first safe camera system for 3D zone monitoring in an industrial environment. Safety on camera systems such as SafetyEYE is no longer based on a strict, physical separation between the process and the operator, but rather on mutual, safe cooperation between man and machine; as such, it opens up new forms of collaboration. The next generation of SafetyEYE will further optimize object resolution, making it easier to design flexible work practices.

Acknowledgments: The reported work of the HiDRaLoN project [12] (High Dynamic Range and Low Noise CMOS-Image-Sensors) at the end of Section 2 was funded by the German Federal Ministry of Education and Research (BMBF), BMBF contract number 16N10370/13N10370, as part of the CATRENE project CA301 HiDRaLoN. We would like to thank BMBF and the CATRENE Office for their support and our colleagues, Heinz-Gerd Graf, Markus Schneider and Astrid Hamala at IMS CHIPS, as well as Daniel Hoberg, Martin Kurth and Sabine Skaletz-Karrer at Pilz and Sabine Strobel for their helpful assistance in putting together this paper.

Received December 14, 2012; accepted March 6, 2013

References

[1] B. Höfflinger, Ed., 'High-Dynamic-Range (HDR) Vision' (Springer, Berlin, 2007).
[2] J. N. Burghartz, H.-G. Graf, C. Harendt, W. Klingler, H. Richter, et al., 'HDR CMOS Imagers and Their Applications', in Proc. 8th IEEE in ICSICT, (Shanghai, China, 2006) pp. 528–531.
[3] U. Seger, U. Apel and B. Hoefflinger. in 'Handbook of Computer Vision and Application', Vol. 1, (Academic Press, San Diego, London) pp. 223–235.
[4] H. G. Graf, B. Höfflinger, U. Seger and A. Siggelkow, Fachzeitschrift Elektronik 3 (1995).
[5] U. Seger, H.-G. Graf and M. E. Landgraf, IEEE Micro 13, 50–56 (1993).
[6] C. Jansson, P. Ingelhag, C. Svensson and R. Forchheimer. Analog Int. Circ. Sig. Proc. 4, 37–49 (1993).
[7] O. Yadid-Pecht and R. Ginosar. IEEE Trans. Electron Dev. 38, 1772–1781 (1991).
[8] EMVA 1288 Standard Release 3.0, in 'Standard for Characterization of Image Sensors and Cameras', EMVA (2010), available at www.emva.org/cms/upload/Standards/Stadard_1288/EMVA1288-3.0.pdf.
[9] Developer Camera RS, www.ims-chips.de/content/pdftext/HDRC-MDC_04_bw_09.pdf.
[10] Developer Camera GS, www.ims-chips.de/content/pdftext/HDRC-MDC_05_09.pdf.
[11] M. Strobel, Proc. SPIE Photonics Europe 8436, 84360H-1–84360H-14 (2012).
[12] HiDRaLoN Project, http://hidralon.eu.
[13] Directive 2006/42/EC of the European Parliament and of the Council of 17 May 2006 on Machinery and Amending Directive 95/16/EC (recast) (Text with EEA relevance).
[14] IEC 61496, Safety of Machinery – Electro-sensitive Protective Equipment – Part 1: General Requirements and Tests, 3ED 2012.
[15] Certificate no. MHHW 07 021, dated 03/01/2011, Berufsgenossenschaft Holz und Metall, Prüf- und Zertifizierungsstelle, Hebezeuge, Sicherheitskomponenten und Maschinen (HSM), Fachbereich Holz und Metall.
[16] B. Ostermann, 'Industrial Jointed Arm Robot Evading Dynamic Objects', Master Thesis, Hochschule Bonn-Rhein-Sieg (2009), http://www.inf.fh-bonn-rhein-sieg.de/informatikmedia/Downloads/Personen/reinert/ostermann.pdf.
[17] Application Report: Flexible Manufacturing of Fuel Cells with SafetyEYE, http://www.pilz.com/imperia/md/content/editors_mm/o-team/application_story_safetyeye_zbt_en.pdf.
[18] Application Report: Robot Welding Station in the Automotive Industry, http://www.pilz.com/imperia/md/content/editors_mm/o-team/application_story_safetyeye_benteler_en.pdf.

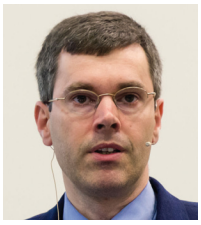

Markus Strobel received a degree in Electrical Engineering (Dipl.-Ing.) from the University of Stuttgart, Germany, and heads the business division Vision at the Institute for Microelectronics Stuttgart (IMS CHIPS). He has been with IMS CHIPS since 1997 and focuses on CMOS imaging, namely the development of high dynamic range CMOS (HDRC) image sensors, optical characterization, optical and electrical test environments, as well as camera systems for industrial, automotive, medical and custom specific applications.

Dietmar Döttling was born in Stuttgart in 1963 and studied Computer Science at Esslingen University. From 1991 to 1999, he was responsible for software development and commissioning of robot systems at Manz Automatisierungstechnik GmbH, Reutlingen. In 1999, Dietmar Döttling joined Pilz GmbH & Co. KG as Project Manager for 'SafetyEYE development'. Since 2008, he has been Head of the Sensor Systems Division at Pilz GmbH & Co. KG.